Ionic Association of Hydroperoxide Anion HO_2^- in the Binding Mean Spherical Approximation. Spectroscopic Study of Hydrogen Peroxide in Concentrated Sodium Hydroxide Solutions

Jerzy Chlistunoff*

Los Alamos National Laboratory, Los Alamos, New Mexico 87544

Jean-Pierre Simonin*

Laboratoire LI2C (UMR 7612), Université Pierre et Marie Curie-Paris 6, Boîte No. 51, 4 Place Jussieu, 75252 Paris Cedex 05, France

Received: September 7, 2006

The ultraviolet−visible (UV−vis) spectroscopy of hydrogen peroxide in concentrated sodium hydroxide solutions was studied. The peroxide band in the UV range shifts from ∼214 nm to ∼236 nm as the NaOH concentration increases from 0.338 mol dm^{-3} to 13.1 mol dm^{-3}. The band originates from an intramolecular electronic transition of the hydroperoxide anion HO_2^-, as indicated by the negligible temperature effect on the band position and confirmed by ab initio quantum mechanical calculations. It is postulated that the bathochromic shift of the peroxide band that accompanies the increase in NaOH concentration originates from the formation of the ion pair ($Na^+HO_2^-$). The equilibrium constant for the ion association reaction (0.048 mol^{-1} dm^3) and the characteristics of the individual absorption bands of the hydroperoxide anion and its associate with Na^+ were determined from the numerical modeling of the absorbance data, using the binding mean spherical approximation (BIMSA).

1. Introduction

Hydrogen peroxide is a versatile, environmentally friendly chemical agent, which exhibits pH-tunable reduction−oxidation (red-ox) properties. For instance, an alkaline solution of hydrogen peroxide is extensively used by the paper and pulp industry as a quality bleaching agent. Attempts have been made to develop electrochemical reactors based on the fuel-cell principle,[1−3] which would produce peroxide in a cleaner, safer, and less-expensive way than the existing antraquinone technology. On the other hand, peroxide is an unwanted byproduct of proton-exchange membrane fuel cells (PEMFCs), because it is most likely responsible for the premature membrane degradation.[4] A significant peroxide generation can also occur in chlor-alkali cells that use oxygen-depolarized cathodes.[5] The unwanted reaction is enhanced by the low water activity in highly concentrated NaOH solutions.[6] While exploring the factors that influence peroxide generation in oxygen-depolarized chlor-alkali cells,[6] we discovered that the ultraviolet (UV) band of peroxide in the highly concentrated NaOH solutions was located at significantly longer wavelengths than the band of hydroperoxide anion that was observed by Muhammad and Rao in an early (and probably only) spectroscopic study of peroxide in an alkaline medium.[7] Because the strong bathochromic shift of the UV band could indicate a change in the peroxide equilibrium, we undertook a systematic study of the peroxide spectrum in NaOH solutions to elucidate the chemistry responsible for the observed phenomenon.

In this paper, we demonstrate that the observed changes in peroxide spectrum in concentrated NaOH solutions result from the ionic association of hydroperoxide anion (HO_2^-) and Na^+. To describe the association quantitatively, we used the binding mean spherical approximation (BIMSA) theory.[8] This model combines the mean spherical approximation (MSA)[9,10] for the description of ion−ion electrostatic interactions with the Wertheim formalism[11] for that of ionic association. It has been applied to associating aqueous electrolyte solutions for representations of experimental activity and osmotic coefficients.[12,13] In the more-recent implementation of BIMSA,[13] the sizes and charges of the ions in the pair could be assumed to be different from those of the free hydrated ions, to account for the effect of dehydration in the pairing process. The latter version was also successfully used to assess the thermodynamic dissociation constant (pK_a) of 3-phenyl-4-benzoylisoxazol-5-one (HPBI) in concentrated solutions of strong acids.[14] Here, the BIMSA is applied to account for the association of Na^+ with both OH^- and HO_2^-.

2. Experimental Section

All NaOH and NaOH + H_2O_2 solutions used for the spectroscopic measurements were prepared using the concentrated NaOH generated in a homemade oxygen-depolarized chlor-alkali cell that was equipped with a platinum-catalyzed oxygen diffusion cathode and an Asahi F4232 specialized chlor-alkali membrane.[6] The advantage of these solutions was their high purity, which guaranteed an increased stability of peroxide and lower UV−vis backgrounds, as compared to the commercially available analytical-grade NaOH. Stock NaOH solutions were standardized by titration with a 1.000 mol dm^{-3} hydrochloric acid (Fisher) against phenolphthalein. The NaOH solutions of lower concentrations were prepared by diluting the respective stock solution to a volume with Millipore water.

Commercially available, 3% hydrogen peroxide solution (Fisher) was standardized by titration with a 0.1000 N (0.02000 mol dm^{-3}) $KMnO_4$ (Fisher) solution.[15] Its average concentration, as determined from five titrations, was 1.001 ± 0.005 mol dm^{-3}.

* To whom correspondence should be addressed. E-mail addresses: jerzy@lanl.gov, sim@ccr.jussieu.fr.

10.1021/jp065852l CCC: $33.50
Published on Web 12/06/2006

The peroxide concentration in the NaOH samples obtained from the electrolysis was determined using a method of Aziz and Mirza,[16] which was based on a decrease of absorption of alkaline $K_3Fe(CN)_6$ solution at 418 nm upon its reaction with peroxide. The method was modified using higher concentrations of NaOH in the reference $K_3Fe(CN)_6$ solution, to reduce the potential effects of NaOH concentration on the $Fe(CN)_6^{3-}$ spectrum when using highly concentrated NaOH solutions. In the original method, the concentration of NaOH in the reference sample was 0.1 mol dm^{-3}, whereas in the present work, it was 0.8 mol dm^{-3}. The higher concentration of NaOH also accelerated the reaction of peroxide with ferricyanide.[16]

Analytical-grade ("Baker analyzed") potassium hexacyanoferrate (III) (J. T. Baker) and certified ACS sodium hydroxide (Fisher), which was used for the spectrophotometric determination of peroxide, according to Aziz and Mirza,[16] were used as received.

The ultraviolet−visible (UV−vis) spectra were measured using a Hewlett−Packard Model 8452A diode array spectrophotometer. The majority of the spectra were measured at an ambient temperature of 20−25 °C. The measurements at higher temperatures were accomplished using thermally pre-equilibrated cuvettes and solutions. Because of the high purity of the NaOH solutions used, no noticeable thermal decomposition of peroxide was observed in times necessary for the sample handling and measuring spectra.

Quantum mechanical calculations for HO_2^-, O_2^{2-}, NaO_2H, and NaOH were performed using HyperChem Pro 7.5 (Hypercube, Inc.) molecular modeling software. The first approximations of equilibrium geometries of the species of interest under vacuum were obtained using the molecular mechanics with an Amber force field.[17] The geometries were further refined using a restricted Hartree−Fock (RHF) ab initio method.[18] In the calculations for hydroperoxide (HO_2^-) and peroxide (O_2^{2-}) anions, the 6-311++g2d2p basis set was used, whereas for the larger NaO_2H and NaOH molecules, the smaller 6-31G** basis set was used. The spectral characteristics for the optimized geometries of the ions and NaO_2H were obtained using a restricted Hartree−Fock method (RHF),[18] using the respective basis sets and the singly excited configuration interaction (CI), employing all occupied and all unoccupied orbitals. The corresponding numbers of occupied and unoccupied orbitals were as follows: 9 and 59 for HO_2^-, 9 and 49 for O_2^{2-}, and 14 and 40 for NaO_2H. Consequently, the resulting number of configurations considered was 1063, 883, and 1121 for HO_2^-, O_2^{2-}, and NaO_2H, respectively.

The effects of hydration on the geometry of HO_2^-, O_2^{2-}, NaO_2H, and NaOH were evaluated using the molecular mechanics (see prior discussion) for the system that consisted of the ion/molecule of interest and 216 water molecules in a cubical box. The initial molecular mechanics optimization of the geometry was followed by a molecular dynamics (MD) simulation, where the system temperature was stepped from 100 K to 300 K and thermally equilibrated for 0.5 ps, and finally by another molecular mechanics calculation for the configuration obtained from the MD simulation. After that, water was removed from the box and another single-point RHF calculation was performed to calculate the single-point energies and the respective spectra.

The convergence limit for all ab initio calculations was 10^{-5}, and the two-electron integrals cutoff was set at 10^{-10}. Both the ab initio and molecular mechanics calculations used a Polak−Ribiere optimizer.

3. Theoretical Section

In this section, we give the main BIMSA relations used for the assessment of hydroperoxide ion association.

Because Na^+ and OH^- are dominant in the solutions studied here (H_2O_2 was introduced in tracer amounts), it was assumed that the concentration of free Na^+ was governed by the association equilibrium between these two species. This association was described following the method described in ref 13.

This feature brings significant simplification to the description of the association of Na^+ and HO_2^-, which was done as follows.

The mass-action law present in the BIMSA model may be expressed as

$$K = \frac{\rho_P}{\rho_1 \rho_2} \mathrm{r} \tag{1}$$

in which K is the thermodynamic association constant for the reaction $Na^+ + HO_2^- \leftrightarrow NaHO_2$. The parameters ρ_1 and ρ_2 are the number densities of free Na^+ and HO_2^-, respectively; ρ_P is that of the pair, ($Na^+HO_2^-$), denoted by the subscript P, and r represents the ratio

$$r \equiv \frac{y_P}{y_1 y_2} \tag{2}$$

with y_i being the activity coefficient of species i.

The quantity r can be calculated in the BIMSA. One has[13]

$$r = \frac{g_{34}^{\infty}}{g_{34}} \exp(-\beta\Delta\mu_1 - \beta\Delta\mu_2 + \beta\Delta\mu_3 + \beta\Delta\mu_4) \tag{3}$$

where g_{34} denotes the contact value of the radial distribution function (RDF) for species 3 and 4 (Na and HO_2 in the pair), respectively, and the superscript infinity symbol (∞) denotes infinite dilution of the solute. The expression of g_{34} can be found in ref 13 (eqs 23−27). Moreover, in eq 3, $\beta \equiv 1/(k_B T)$ (where k_B is the Boltzmann constant and T is the temperature) and $\Delta\mu_i$ denotes the excess chemical potential of species i, which is given by

$$\beta\Delta\mu_i = \beta\Delta\mu_i^{HS} + \beta\Delta\mu_i^{el} - \rho_P \frac{\partial \ln g_{34}^{HS}}{\partial \rho_i} \tag{4}$$

in which the superscripts "HS" and "el" indicate hard sphere and electrostatic contributions, respectively. The expressions of $\beta\Delta\mu_i^{HS}$ and $\beta\Delta\mu_i^{el}$can be found in ref 19 (in the term M_i of eq 30 and the first term of eq 19, respectively). Notice that the contribution of the last term of eq 4 is small, because the total concentration of hydroperoxide ion was low in the experiments.

The proportion of free HO_2^-, $x_2 = \rho_2/(\rho_2 + \rho_P)$, can be obtained easily from eq 1. One gets the simple result

$$x_2 = \frac{1}{1 + K\rho_1/r} \tag{5}$$

in which r is given by eq 3 and ρ_1, which is the number density of free Na^+, is computed within the BIMSA, using the results of ref 13 for binary NaOH solutions.

One notices that eq 5 is an implicit equation in x_2, because the latter is also present in r (through the quantity ρ_P in eq 4, and in the expressions of $\beta\Delta\mu_i^{HS}$ and $\beta\Delta\mu_i^{el}$). The speciation of the hydroperoxide ion was computed numerically by solving eqs 3−5, using an iterative procedure. However, because the

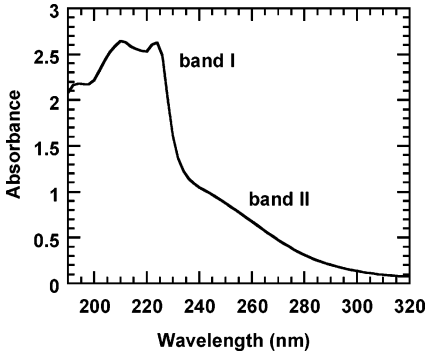

Figure 1. Spectrum of the 11.2 mol dm^{-3} (29.2%) NaOH solution generated in a chlor-alkali cell with an oxygen-diffusion cathode.

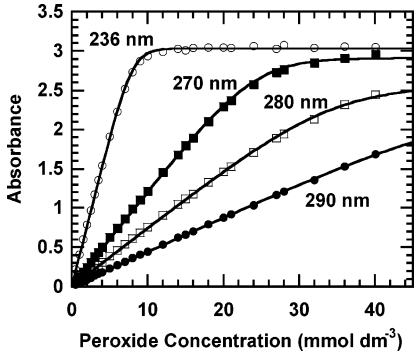

Figure 2. Absorbance of hydrogen peroxide solutions in 0.676 mol dm^{-3} NaOH at selected wavelengths, corrected for the background absorbance measured for pure NaOH solution.

total concentration of hydroperoxide ion was low in the experiments, all terms that contain ρ_P could be equally neglected without a sensitive loss of accuracy.

4. Results

4.1. Spectra of NaOH Solutions. The typical spectrum of a NaOH solution generated in one of our chlor-alkali cells is shown in Figure 1. The positions of the UV cutoff (band I) in our solutions and the solutions that contain identical concentrations of commercial NaOH were indistinguishable. Band I was attributed to the charge-transfer-to-solvent (CTTS) transition of the hydroxide anion.[20] Because of the stray light, the maximum absorbance measured for this band attained a value of ~2.7 (Figure 1), irrespective of the NaOH concentration.

Band II was attributed to the hydroperoxide anion HO_2^-, which is the predominant form of hydrogen peroxide in alkaline media.[7,21] The presence of a roughly linear correlation between the intensity of band II and the determined concentration of peroxide strongly supported such an assignment, even though band II was located at noticeably longer wavelengths than the peroxide band observed by Muhammad and Rao.[7] Band II could not be attributed to the impurities of NaOH, which may have been transferred through the membrane from the anode compartment, such as chloride and chlorine oxo-anions. Chloride and chlorate, which are the two most likely impurities of NaOH generated in a membrane process,[22] as well as perchlorate, absorb in the far-UV region,[20,23,24] and their molar absorptivities at 220 nm are very low. The spectrum of hypochlorite exhibits a band in the near UV region, but the band is centered at 292 nm,[25,26] i.e., at significantly longer wavelengths than the band that we observed. Among the absorption bands of chlorine oxo-anions, the chlorite band at 260 nm with the molar extinction coefficient of ~159[24,27] seems closest to the band that we observed. However, chlorite is rather an uncommon impurity of NaOH from the membrane electrolysis, most likely because it reacts with hypochlorite[28] and, thus, cannot accumulate in the brine and travel across the membrane to the cathode compartment.

As expected for the inherently unstable hydrogen peroxide, the intensity of band II slowly decreased over time and the band would eventually disappear after several hours to a few days. The spectrum of the solution taken after the disappearance of band II exhibited a lower baseline absorbance than the spectrum of a NaOH solution of comparable concentration prepared using the commercial product and, thus, indicated a higher purity of NaOH generated in our cells. In accordance with the aforementioned finding, the alkaline solutions of hydrogen peroxide prepared using our NaOH exhibited a higher stability than those obtained using the commercial product.

4.2. Stray Light Effects. To quantify the stray light effects on the measured absorbance of peroxide, the spectra of two NaOH solutions (0.676 and 8.12 mol dm^{-3}) that contained several concentrations of peroxide were measured. We observed that the absorbance increased linearly with peroxide concentration up to a factor of ~2, whereas a noticeable negative departure from the Lambert−Beer law could be observed at higher optical densities. Eventually, the measured absorbance stopped changing with the peroxide concentration and reached a weakly wavelength-dependent limiting value of ~3 (Figure 2). The maximum absorbance of ~3 reflects exclusively the amount of stray light reaching the detector and carries no information on the light absorption by the sample.[29] It can be used to calculate the intensity of stray light at a given wavelength and the corresponding negative absorbance errors resulting from the stray light.

The limiting absorbance and, hence, the absorbance errors could not be directly determined for the longer wavelengths studied (Figure 2), because the slow decomposition of peroxide led to the formation of small oxygen bubbles in the solutions that contained the required peroxide concentrations. In such cases, the limiting absorbance was obtained from a numerical fitting of the absorbance versus concentration plots shown in Figure 2. The following equation was used to fit the data:[29]

$$A_{meas}(\lambda) = -\log(10^{-\epsilon(\lambda)C\delta} + B) \qquad (6)$$

The parameter B in eq 6 is the ratio of intensity of the stray light to that of the incident light (I_{stray}/I_0) and is assumed to be constant at a given wavelength; ϵ is the molar extinction coefficient, C is the molar concentration of peroxide, and δ is the cuvette thickness. The term $\epsilon(\lambda)C\delta$ represents the absorbance that would be measured in the absence of stray light.

The relative absorbance errors that result from the stray light for 2.00 mmol dm^{-3} peroxide concentration at two different NaOH concentrations and four selected wavelengths are plotted in Figure 3. Although the errors of −1.3% and −2.7% at 290 nm (Figure 3) determined for 8.12 mol dm^{-3} and 0.676 mol dm^{-3} NaOH, respectively, may seem relatively high, one must note that the absolute absorbance errors for this peroxide concentration were never higher than 0.004 and, for most wavelengths, did not exceed 0.002. Because a variety of phenomena can lead to significantly higher errors, we concluded that the spectra obtained for 2.00 mmol dm^{-3} peroxide were sufficiently accurate and we selected this concentration for further studies.

4.3. Effects of NaOH Concentration on the HO_2^- Band. The UV cutoff shifted from ~220 nm to ~230 nm when the NaOH concentration was increased from 0.338 mol dm^{-3} to

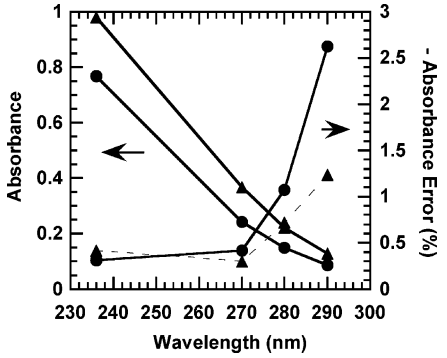

Figure 3. Measured absorbance, and its relative error resulting from stray light, for 2.00 mmol dm^{-3} peroxide in (●) 0.676 mol dm^{-3} NaOH and (▲) 8.12 mol dm^{-3} NaOH.

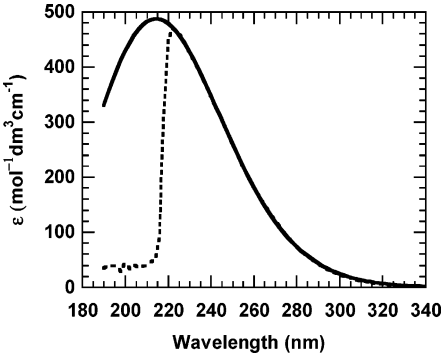

Figure 4. Molar absorptivity of peroxide in 0.338 mol dm^{-3} NaOH obtained from the experimental spectrum of 2.00 mmol dm^{-3} peroxide (- - -) corrected for the background (NaOH) absorption and (—) from the numerical fitting using the semilogarithmic Gaussian function (eq 9). The sudden drop of the absorptivity at $\lambda < 220$ nm results from the failure of the background correction, resulting from the stray light.

13.1 mol dm^{-3} (ca. 15 mol/kg). Despite the shift, the peroxide band seemed to be better separated from the OH^- band in more-concentrated NaOH solutions. Because of the substantial stray light effects at the wavelengths corresponding to the UV cutoff, our attempts to extract the peroxide band from the measured spectra by subtracting the absorbance of pure NaOH solution failed (Figure 4). Quite predictably, numerical procedures to determine the individual components that correspond to OH^- and HO_2^- also failed. The approximate spectral parameters that characterize the peroxide band were thus obtained from a numerical fitting of its long-wave portion measured for the 2.00 mmol dm^{-3} peroxide solutions. The short-wave limit of the respective wavelength range was dependent on the NaOH concentration and typically corresponded to the measured absorbance of 1.1−1.2. The stray light errors in this range were still negligible and the corrections for NaOH absorption were small and, thus, considered accurate. At the same time, a significant portion of the band at wavelengths shorter than that of its lower-energy inflection point was included in the analysis, thus making the numerical fitting more reliable. Three different Gaussian functions were attempted:

$$A_{\text{meas}} = \epsilon(\lambda_{\max}) C\delta \exp\left[-\gamma\left(\frac{1}{\lambda_{\max}} - \frac{1}{\lambda}\right)^2\right] \quad (7)$$

$$A_{\text{meas}} = \epsilon(\lambda_{\max}) C\delta \exp[-\gamma(\lambda_{\max} - \lambda)^2] \quad (8)$$

$$A_{\text{meas}} = \epsilon(\lambda_{\max}) C\delta \exp\left\{-\gamma\left[\ln\left(\frac{\lambda}{\lambda_{\max}}\right)\right]^2\right\} \quad (9)$$

The parameter γ in eqs 2−4 is a measure of the band broadness

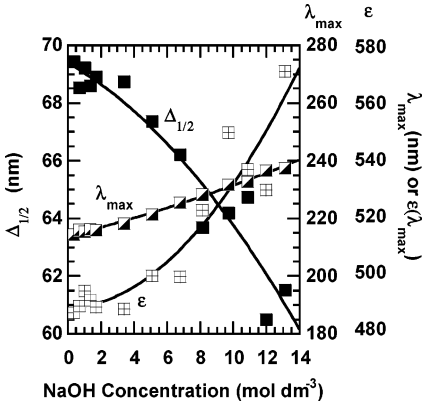

Figure 5. Dependence of the parameters characterizing the peroxide band obtained from the numerical fitting of the spectra, using the semilogarithmic Gaussian function.

and is defined differently for each function. The semilogarithmic Gaussian function (eq 9) was determined to consistently produce the best fits. The best semilogarithmic fit of the peroxide spectrum in 0.338 mol dm^{-3} NaOH is shown in Figure 4. The corresponding band parameters, $\lambda_{\max}$, $\epsilon(\lambda_{\max})$, and the bandwidth at the half-height ($\Delta_{1/2}$), obtained from the numerical fitting, are shown in Figure 5. For the semilogarithmic Gaussian function, the parameter $\Delta_{1/2}$ is given by

$$\Delta_{1/2} = 2\lambda_{\max} \sinh\left(\sqrt{\frac{\ln 2}{\gamma}}\right) \quad (10)$$

The plots in Figure 5 demonstrate that the strong bathochromic shift of peroxide band is accompanied by an increase in the band intensity and a decrease in its width. The observed effects may indicate the presence of a NaOH-concentration-dependent equilibrium that involves HO_2^-, or the CTTS character[30] of the electronic transition in question, or both. This issue is further discussed in the next two sections.

4.4. Effect of Temperature and Dielectric Constant on Peroxide Spectrum. Although the high sensitivity of peroxide spectrum to NaOH concentration may indicate its CTTS character, the low intensity of the band may suggest otherwise, because the majority of CTTS transitions are characterized by high oscillator strengths. However, for a small number of CTTS transitions, quite low intensities were reported.[20] Our estimates of the energy of the hypothetical CTTS transition for HO_2^- indicated that the relatively low energy of the peroxide band was not excluding its CTTS character either. The correlation of the CTTS energies with the redox potentials of the corresponding radicals for a series of anions[31,32] led to a value of 238 nm for the wavelength of the hypothetical CTTS transition for HO_2^-, which is quite close to the measured wavelength of the peroxide band. More rigorous estimates within the framework of the diffuse model of the CTTS phenomena[20,33−35] using the published vertical ionization potential of HO_2^- (see ref 36) and the estimated range for crystal radius of HO_2^- produced even a longer wavelength for the transition, namely 304 and 402 nm for its lower and upper, crystal-radius-dependent limit. To unequivocally determine the nature of the peroxide electronic transition, we decided to examine the effect of temperature on the peroxide spectrum. Unlike intramolecular transitions, CTTS transitions are sensitive to temperature changes and exhibit a significant bathochromic shift that is caused by a temperature increase.[20]

Spectra of 2.00 mmol dm^{-3} peroxide in 0.676 mol dm^{-3} NaOH were measured at different temperatures, ranging from

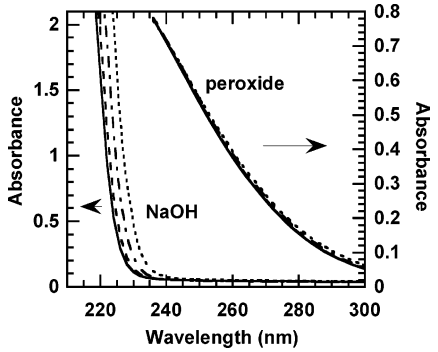

Figure 6. Temperature effect on the peroxide and OH^- bands: (—) 25 °C, (- - -) 32 °C, (— - —) 48 °C, and (• • •) 70 °C.

25 °C to 70 °C. The results of these experiments are shown in Figure 6. As expected, the UV cutoff (CTTS band of OH^-) shifts significantly toward the longer wavelengths when the temperature increases; however, the peroxide band position remains constant within 1 nm, thus indicating an intramolecular character of the transition.

The intramolecular nature of the peroxide band, which was further supported by the quantum mechanical calculations (see below), suggests that the observed changes in peroxide spectrum result from a chemical equilibrium that involves the hydroperoxide anion. Based on the concentration argument, the most likely processes that involve HO_2^- in highly concentrated NaOH solutions are the ionic association and the abstraction of the second H^+ cation. The second acid dissociation of hydrogen peroxide seems relatively less likely, because this reaction is highly endothermic ($\Delta H° \approx 100$ kcal/mol)[21] and its expected equilibrium constant is extremely low. On the other hand, the ionic association of HO_2^- is very probable, based on the comparison with OH^-, which forms strong associates with the Na^+ cation.[12,37,38] To verify the ion association hypothesis, we examined the effect of methanol on the peroxide spectrum. We determined that the peroxide band measured for 0.338 mol dm^{-3} NaOH in a mixture of ~84% methanol (by volume) and ~16% water was shifted by ~10 nm toward the longer wavelengths, as compared to the respective aqueous solution. At the same time, the band intensity decreased by ~30%. Although the observed shift of the peroxide band cannot be indisputably attributed to an increase in ionic association, it is in the same direction as the shift resulting from an increase in NaOH concentration, which remains in agreement with the expected effect of the lower dielectric constant of the methanol/water mixture[39] on the ion association of hydroperoxide.

4.5. Quantum Mechanical Calculations. *4.5.1. Spectra of HO_2^- and O_2^{2-}.* The calculated ground-state configurations of HO_2^- and O_2^{2-} are $(1a')^2(2a')^2(3a')^2(4a')^2(5a')^2(1a'')^2(6a')^2(7a')^2(2a'')^2$ and $(1\sigma_g)^2(1\sigma_u)^2(2\sigma_g)^2(2\sigma_u)^2(1\pi_u)^4(3\sigma_g)^2(1\pi_g)^4$, respectively. The spin-allowed transitions with nonzero oscillator strengths, calculated for hydroperoxide and peroxide anions under vacuum and in aqueous solution, are listed in Table 1. The data in Table 1 also include the relatively strong electronic transitions in the lower-energy vacuum UV region, which may have slightly contributed to the measured absorbance.

Based on the data in Table 1, it can be postulated that the peroxide band most likely originates from the $2a'' \rightarrow 9a'$ electronic transition in HO_2^-. The extrapolation of the measured peroxide band to zero ionic strength, followed by the numerical integration, leads to a wavelength of 213.8 nm and an oscillator strength of 0.0149 for the resulting band, whereas the calculated wavelength and oscillator strength for the $2a'' \rightarrow 9a'$ transition are 217.17 nm and 0.0280, respectively. The oscillator strength

TABLE 1: Calculated Electronic Transitions of Hydroperoxide (HO_2^-) and Peroxide (O_2^{2-}) Anions

λ_{max} (nm)	oscillator strength[a]	transition[b]	remark
		HO_2^- in vacuo	
325.96	0.0003	$2a'' \rightarrow 8a'$	
263.99	0.0003	$7a' \rightarrow 8a'$	
246.70	0.0052	$2a'' \rightarrow 9a', 16a'$	
217.36	0.0120	$7a' \rightarrow 9a', 16a'$	
		HO_2^- in water	
466.12	0.0003	$2a'' \rightarrow 8a'$	
333.56	0.0070	$7a' \rightarrow 8a'$	
217.17	0.0280	$2a'' \rightarrow 9a'$	
186.14	0.0434	$7a' \rightarrow 9a'$	
		O_2^{2-} in vacuo	
348.50	0.0245 (0.0490)	$1\pi_g \rightarrow 3\sigma_u$	doubly degenerate
185.17	0.3592	$1\pi_g \rightarrow 1\pi_u$	
		O_2^{2-} in water	
442.88	0.0330 (0.0660)	$1\pi_g \rightarrow 3\sigma_u$	doubly degenerate
233.61	0.1569	$1\pi_g \rightarrow 2\pi_u$	

[a] Values in parentheses represent the total oscillator strength for the degenerate transitions. [b] Expressed using ground-state orbitals that predominantly contribute to the transition.

of the weaker $7a' \rightarrow 8a'$ transition (Table 1) seems to be overestimated, because the measured spectra exhibited virtually no light absorption at ~333 nm.

The results of quantum mechanical calculations for O_2^{2-} (Table 1) do not provide proof that the NaOH-concentration-driven changes in the peroxide spectrum result from the ionic association rather than the formation of the peroxide anion O_2^{2-} at high NaOH concentrations. The dry or partially hydrated mixtures of solid sodium peroxide and sodium hydroxide have a yellowish color,[40] which seems to remain consistent with the calculated wavelength (442 nm) and oscillator strength (0.0660) of the $1\pi_g \rightarrow 3\sigma_u$ transition (see Table 1). However, the most-concentrated NaOH solutions used in this work that contain peroxide never exhibited a yellowish coloration. Also, the crystals of hydrated sodium peroxide ($Na_2O_2 \cdot 8H_2O$) are colorless,[41] which may suggest that the wavelength of the $1\pi_g \rightarrow 3\sigma_u$ transition and/or its oscillator strength obtained from the calculations may be overestimated. If this is the case, the changes in peroxide spectrum resulting from the increase in NaOH concentration might result from the growth of the strong $1\pi_g \rightarrow 2\pi_u$ band at ~234 nm (see Table 1), accompanying the formation of minute quantities of hydrated O_2^{2-}. Nevertheless, as mentioned previously, such a hypothesis must be treated with caution, because of the extremely low expected value of the second acid dissociation constant of hydrogen peroxide.[21] Additional support for the ion association hypothesis was obtained from the quantum mechanical calculations for the NaO_2H molecule described in the next section.

4.5.2. NaOH and NaO_2H Molecules. Figure 7 shows the optimized geometries and charge densities of NaO_2H and NaOH molecules under vacuum and in water. Both molecules assume higher symmetry under vacuum than in solution. Although the NaOH molecule is linear under vacuum (C_∞ point group) and NaO_2H is planar (C_s group), their respective symmetry groups in water become C_s and C_1, respectively (Figure 7). The symmetry changes that result from hydration are accompanied by significant changes in the bond lengths and angles. The Na−O bond stretches upon hydration from 1.920 Å to 2.235 Å in NaOH and from 2.070 Å to 2.252 Å in NaO_2H (see the Na−O(2) bond in Figure 7). Similarly, the O−H bond in NaOH stretches from 0.938 Å to 0.971 Å and from 0.939 Å to 0.984 Å in NaO_2H (see the H−O(1) bond). The O−O bond in NaO_2H contracts from 1.477 Å under vacuum to 1.325 Å in water. In

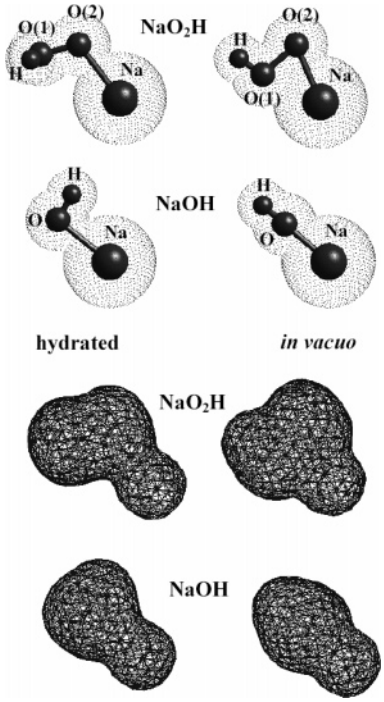

Figure 7. Geometries of NaOH and NaO_2H molecules (top) and their total charge densities (bottom) obtained from molecular mechanics and ab initio calculations (see text). The charge density contour value is 0.005.

the NaO_2H molecule, the Na−O−O angle increases from 70.53° to 112.69°, the H−O−O angle increases from 103.39° to 108.99°, and the torsion Na−O−O−H angle changes from 180° (planar molecule) to 89.34° upon hydration. Also, the charge of the Na atom in the NaO_2H molecule decreases upon hydration from 0.789 to 0.746. The observed changes in the equilibrium geometries of the molecules remain in agreement with the intuitively expected effects that a polar solvent would have on the polar Na−O and H−O bonds and how these effects would influence the geometry of the molecules.

The classical character of molecular mechanics calculations does not allow one to identify the calculated geometries of hydrated NaOH and NaO_2H molecules with the actual geometries of the respective ionic associates in aqueous solutions. However, the calculated geometries are believed to reasonably approximate the true geometries of the associates in solution. Consequently, to obtain the approximate spectral characteristics of ($Na^+HO_2^-$) and evaluate the effects of ion pairing on the HO_2^- spectrum, we performed RHF ab initio calculations for the optimal geometries of NaO_2H under vacuum and in solution (see Figure 7). The calculated spin-allowed transitions with nonzero oscillator strengths are listed in Table 2.

The data in Table 2 demonstrate that the UV spectrum of NaO_2H under vacuum is dominated by the 11a′ → 12a′ transition at 217.67 nm with an oscillator strength of 0.0192. The spectrum of NaO_2H in solution exhibits at least four relatively strong electronic transitions in the non-high-vacuum UV range. These are the 14a → 15a, 13a → 15a, 13a → 16a, and 13a → 17a transitions, at 431.26, 347.07, 238.91, and 230.91 nm, respectively. All these transitions are located at significantly longer wavelengths than the 2a″ → 9a′ transition in hydrated HO_2^- (217.17 nm, Table 1) and the 11a′ → 12a′ transition in NaO_2H under vacuum (217.67 nm, Table 2). The analysis of orbital shapes revealed that the strong electronic transitions in NaO_2H in vacuo and in solution correspond to the transfer of electrons from an antibonding π molecular orbital predominantly localized on O atoms to an orbital predominantly localized on the Na atom. This observation demonstrates that the formation of ($Na^+HO_2^-$) in concentrated NaOH solutions is likely to cause the bathochromic shift of the peroxide band if the geometry of the pair resembles that of hydrated NaO_2H from the molecular mechanics calculations.

TABLE 2: Calculated Electronic Transitions of NaO_2H in Different Environments

λ_{max} (nm)	oscillator strength	transition[a]
	in vacuo	
266.01	0.0025	3a″ → 12a′
250.83	0.0006	3a″ → 13a′, 19a′
217.67	0.0192	11a′ → 12a′
208.02	0.0058	11a′ → 13a′, 19a′
199.66	0.0074	3a″ → 4a″
192.58	0.0014	3a″ → 14a′
186.98	0.0080	3a″ → 13a′, 19a′
	water	
431.26	0.0326	14a → 15a
347.07	0.0107	13a → 15a
293.39	0.0072	14a → 16a
281.98	0.0027	14a → 17a
250.92	0.0006	14a → 18a, 19a
238.91	0.0110	13a → 16a
230.91	0.0269	13a → 17a
211.79	0.0030	13a → 18a, 19a
187.53	0.0102	14a → 19a

[a] Expressed using ground-state orbitals that predominantly contribute to the transition.

4.6. Ionic Association of Hydroperoxide Anion. The results presented in the previous sections strongly suggest that the bathochromic shift of the peroxide band originates from the formation of ionic associates between HO_2^- and Na^+. Unfortunately, the determination of the number and spectral characteristics of the species that contribute to the peroxide spectrum is not easy. This is because the methods commonly used for such purposes, e.g., the singular-value decomposition (SVD) method,[42] are not readily applicable in the present case, because the changes in peroxide spectrum are accompanied by the changes in ionic association of NaOH,[12,37,38] water activity,[43] and ionic activity coefficients. In our initial attempts to determine the number and spectral characteristics of different peroxide species, a numeric procedure was used to deconvolute the spectra into several Gaussian components. The results of the deconvolution using two Gaussian components remained in an approximate agreement with the model, assuming the formation of the ion pair. The deconvolution using three Gaussian components also suggested the presence of two major species in the equilibrium. However, the differences between the results obtained in both cases, as well as the overall scatter of data, made the conclusions questionable. Using four different components in the analysis produced meaningless results and the method was eventually abandoned.

Consequently, it was assumed, in further analysis, that only two peroxide species, HO_2^- and ($Na^+HO_2^-$), contributed to the equilibrium and the measured spectra. In addition to peroxide, the following species were considered in the assumed model of equilibrium: "free" OH^- and Na^+ ions as well as (Na^+OH^-) ion pairs.

4.6.1. Application of the BIMSA to Ionic Association of HO_2^-. To facilitate the BIMSA simulations, a few assumptions and approximations were implemented. First of all, it was assumed that the low concentration of peroxide in the studied solutions did not affect the association of NaOH. Consequently, the concentrations of Na^+, OH^-, and (Na^+OH^-) in the studied solutions were obtained using the same approach and input

parameters as in the previous study.[13] Namely, the diameter of the hydrated OH^- ($\sigma_{2(OH^-)}$) was 3.55 Å and that of the hydrated Na^+ ($\sigma_{1(Na^+)}$) was given by the formula[12,13]

$$\sigma_{1(Na^+)}\,(\text{Å}) = 3.87 - 0.05033 C_{NaOH}(\text{mol dm}^{-3})$$

The parameter values for the ions in the (Na^+OH^-) pair were as follows. The diameters were 3.797 Å for Na ($\sigma_{3(Na(Na^+OH^-))}$) and 3.40 Å for OH ($\sigma_{4(OH(Na^+OH^-))}$),[13] respectively; the charge of Na, $z_{3(Na(Na^+OH^-))}$, was 0.758.[13] The association constant for NaOH, K^{ass}_{NaOH}, was 0.2805 mol^{-1} dm^3 (see ref 13) and the extinction coefficients for "free" hydroperoxide ion were those measured for 2.00 mmol dm^{-3} peroxide in 0.338 mol dm^{-3} NaOH.

To reduce the number of adjustable parameters, the charge of Na in the ($Na^+HO_2^-$) ion pair, $z_{3(Na(Na^+HO_2^-))}$, and the diameter of "free" HO_2^-, $\sigma_{2(HO_2^-)}$, were assigned constant numeric values. The charge of Na in the pair, $z_{3(Na(Na^+HO_2^-))}$, was determined to be 0.746 (see Section 4.5.2). It must be mentioned that the results are slightly sensitive to the value of this parameter. Therefore, a 10% change in its value produced, on average, a change of ~0.5% in the calculated extinction coefficient of the ion pair. Similarly, the fit results were marginally sensitive to the choice of diameter of "free" HO_2^-, $\sigma_{2(HO_2^-)}$. The fits performed for the various wavelengths used experimentally (230−274 nm) gave a mean value for $\sigma_{2(HO_2^-))}$ of 5.3 Å. This value resulted in a good agreement between the concentrations of ($Na^+HO_2^-$) obtained directly from the modeling and from the subsequent numerical deconvolution of the spectra, using the extinction coefficients from the modeling. Moreover, it was assumed that the diameters of Na ($\sigma_{3(Na(Na^+HO_2^-))}$) and HO_2 ($\sigma_{4(OH(Na^+HO_2^-))}$) in the pair were equal.

Consequently, the adjustable parameters in the simulations were as follows: the association constant of ($Na^+HO_2^-$), $K^{ass}_{NaHO_2}$; the extinction coefficients of the pair, $\epsilon_{(Na^+HO_2^-)}(\lambda)$; and the equal diameters of Na and HO_2 in the pair, $\sigma_{3(Na(Na^+HO_2^-))} = \sigma_{4(HO_2(Na^+HO_2^-))}$.

When no other constraints were applied, the association constant was determined to decrease slightly as the wavelength increased. To remove this inconsistency, the fitting procedure was conducted as follows. First, a single value of $K^{ass}_{NaHO_2}$ was determined that produced low and comparable deviations of the fit at all wavelengths. From the fits at different wavelengths, the average value of the radius of the Na atom in the pair, $\sigma_{3(Na(Na^+HO_2^-))}$ ($\sigma_{3(Na(Na^+HO_2^-))} = \sigma_{4(HO_2(Na^+HO_2^-))}$), then was obtained and subsequently used to determine the extinction coefficients of the ion pair.

The aforementioned fitting procedure was applied in the entire range of NaOH concentrations, i.e., up to 13.1 mol dm^{-3} (~15 mol/kg); however, the quality of fit substantially deteriorated when concentrations of >9.7 mol dm^{-3} (~10.5 mol/kg) were included in the simulations. The decrease in fit quality was attributed to a systematic error, because it was accompanied by a significant increase in the association constant. The calculations performed for the NaOH concentrations that did not exceed 9.7 mol dm^{-3} resulted in the following values: $K^{ass}_{NaHO_2}$ = 0.048 mol^{-1} dm^3 for the association constant and $\sigma_{3(Na(Na^+HO_2^-))} = \sigma_{4(HO_2(Na^+HO_2^-))} = 4.15$ Å for the diameters of species in the pair.

In Figure 8, the mole fractions of hydroperoxide in its "free" and associated forms obtained from the BIMSA modeling (230 − 274 nm) are shown. Also plotted in Figure 8 are the weighting factors *X* and *Y* obtained from the fitting of the measured spectra using two Gaussian bands, corresponding to the "free" and associated hydroperoxide anions (see section 4.6.2). Although the BIMSA modeling was limited to the narrow range of wavelengths (230−274 nm), where the accurate absorbance measurement was possible for all the NaOH concentrations, a wider wavelength range (NaOH-concentration-dependent) could be used in the latter procedure (see sections 4.2 and 4.3). The measured spectrum was expressed by the following equation:

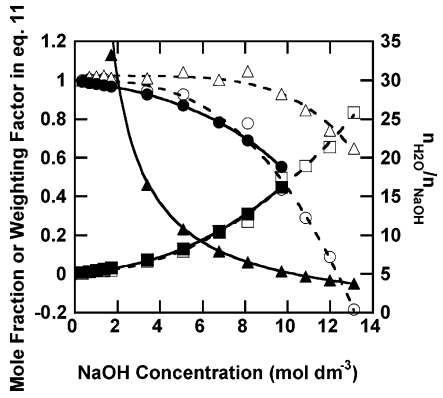

Figure 8. Speciation diagram for 2.00 mmol dm^{-3} hydrogen peroxide in concentrated NaOH solutions, showing the mole fractions from the BIMSA fitting at 230−274 nm ((●) HO_2^- and (■) ($Na^+HO_2^-$)) and the weighting factors in eq 11 (see text) ((○) *Y* (HO_2^-), (□) *X* (($Na^+HO_2^-$)), and (△) $X + Y$). The molar ratio of water to NaOH (n_{H_2O}/n_{NaOH}) is represented by closed triangles (▲).

$$\epsilon(\lambda) = X\epsilon_{(Na^+HO_2^-)}(\lambda) + Y\epsilon_{HO_2^-}(\lambda) \qquad (11)$$

The individual bands in eq 11 were expressed by the semilogarithmic Gaussian functions that best-approximated the spectra of individual components (see section 4.3). To verify the viability of the assumption that only two species contributed to the measured peroxide spectra, the weighting factors *X* and *Y* in eq 11 were allowed to vary independently, so that their sum was not constrained to unity. As shown in Figure 8, the weighting factors *X* and *Y* are very close to the mole fractions obtained from the BIMSA modeling ($1 - x_2$ and x_2, respectively, with x_2 being given by eq 5) and their unrestricted sum is close to unity for NaOH concentrations up to 9.7 mol dm^{-3}, despite the significantly wider wavelength range used in the numerical spectra deconvolution. This observation indicates that the assumption of only two species contributing to the measured absorbance in this concentration range was justified.

A variety of factors may be responsible for the significant departure of the sum of weighting factors from unity at NaOH concentrations of >9.7 mol dm^{-3} and the negative contributions from HO_2^- (a negative *Y* weighting factor) to the measured absorbance at the highest NaOH concentrations (see Figure 8). For instance, the formation of another peroxide species such as a higher ionic associate or peroxide anion O_2^{2-} may be responsible. Moreover, significant dehydration effects do occur at such high NaOH concentrations. As shown in Figure 8, the molar ratio of water to NaOH in these solutions becomes <5 (see Figure 8), which indicates that there is not enough water to fully populate the first coordination spheres of all the ions. Finally, the accuracy of the absorbance measurement at the highest NaOH concentrations was most likely reduced, because of the difficulty of mixing a small quantity of the low-viscosity H_2O_2 solution with a huge excess of the highly viscous NaOH and the resulting accelerated peroxide decomposition under such conditions.

4.6.2. Individual Spectra of HO_2^- and ($Na^+HO_2^-$). To obtain the band parameters for ($Na^+HO_2^-$), the extinction coefficients

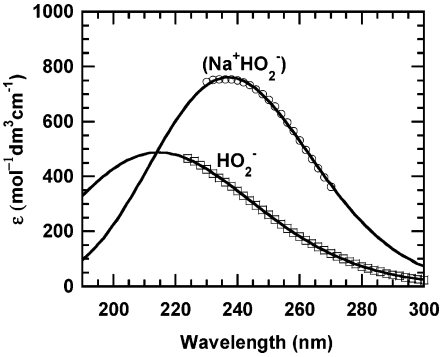

Figure 9. Molar absorptivities of HO_2^- and ($Na^+HO_2^-$) from the BIMSA fitting of the apparent molar absorptivity of hydrogen peroxide. Solid lines represent the best semilogarithmic Gaussian fits of the individual bands (see text).

TABLE 3: Electronic Transitions of Hydroperoxide (HO_2^-) and Peroxide (O_2^{2-}) Anions from the BIMSA Fitting

λ_{max} (nm)	$\epsilon(\lambda_{max})$ (mol^{-1} dm^3 cm^{-1})	$\Delta_{1/2}$ (nm)	γ	f^a	remark
		HO_2^-			
214.4 ± 0.2	487 ± 2	69.4	26.7 ± 0.2	0.0149	eq 9
		$Na^+HO_2^-$			
237.0 ± 0.3	761 ± 2	60.7	42.5 ± 1.0	0.0223	eq 9
236.7 ± 0.2	759 ± 1	64.8	(6.6 ± 0.1) × 10^{-4}		eq 8

[a] Oscillator strength.

between 230 nm and 274 nm obtained from the BIMSA modeling were fitted with the Gaussian functions previously used (eqs 7−9). The fit quality was worst when the inverse linear Gaussian function (eq 7) was used. Of the two remaining functions, the linear Gaussian function (eq 8) produced somewhat better fits; however, the differences in actual band parameters obtained from the linear Gaussian and the semilogarithmic Gaussian fitting (eq 9) were rather small. On the other hand, a better agreement between the weighting factors in eq 11 and the mole fractions of peroxide species from the BIMSA was observed, when the semilogarithmic Gaussian function was used to describe the spectrum of the pair (see section 4.6.1, Figure 8). Consequently, we cannot recommend a particular choice of one of these functions. The HO_2^- and ($Na^+HO_2^-$) bands are shown in Figure 9, and their respective parameters obtained from the fitting are listed in Table 3. For the ion pair, two sets of parameters are given, corresponding to the two functions that produced the fits of comparable quality.

In accordance with the observed changes in peroxide spectrum, the ($Na^+HO_2^-$) band is narrower and located at longer wavelengths than the HO_2^- band. The molar extinction coefficient $\epsilon(\lambda_{max})$ of the ($Na^+HO_2^-$) band and the estimated oscillator strength of the respective transition are also higher than the corresponding numbers obtained for the hydroperoxide anion. The wavelength and the oscillator strength of the ($Na^+HO_2^-$) band are comparable to the respective numbers obtained from the ab initio calculations for the 13a → 16a and 13a → 17a transitions in the hydrated NaO_2H molecule (see Table 2).

Discussion

The association constant of ($Na^+HO_2^-$) determined in this work is a factor of ∼6 lower than the association constant of NaOH.[13] Because the bonding in both associates is predominantly ionic, the stronger association of Na^+ with OH^- than that with the larger HO_2^- seems justified. As could be expected, the adjusted diameter of free HO_2^- (5.3 Å) is larger than that of OH^- (3.55 Å). The same conclusion holds for the average diameter of Na and HO_2 in the pair (4.15 Å) as compared to ca. 3.6 Å for the (Na^+OH^-).

As mentioned in section 4.6.2, the changes in the peroxide spectrum at NaOH concentrations of >9.7 mol dm^{-3} may result from a variety of factors, including the formation of higher ionic associates, dehydration, and, less likely, the formation of doubly ionized peroxide. Although the formation of higher ionic associates and the dehydration of all solutes present in concentrated NaOH are expected to occur simultaneously, one must note that the dehydration alone can produce changes in the peroxide spectrum. The dehydration can modify the peroxide spectrum by directly changing the distances and the strength of interactions between water molecules and hydroperoxide anion and between water and the ion pair, as well as between the ions in the pair. Such phenomena are highly likely to result in NaOH-concentration-driven changes in the quantum energy levels of both "free" and associated hydroperoxide anion and, thus, result in such changes in the peroxide spectrum that cannot be taken into account by a simple equilibrium model of two species with concentration-independent spectra. The difficulties that we encountered when trying to deconvolute the peroxide spectra into individual components may have been caused by phenomena of this type.

Conclusion

In summary, it has been demonstrated that the binding mean spherical approximation (BIMSA) is an effective tool, not only for the determination of ionic association constants in mixtures of electrolytes but it is also helpful in the analysis of electronic spectra of ionic species at high ionic strengths. Specifically, the application of BIMSA in this work made it possible to detect different phenomena that contribute to the bathochromic shift of the hydrogen peroxide band in NaOH solutions. Changes in the peroxide spectrum, up to 9.7 mol dm^{-3} NaOH, can be fully explained by the changes in the relative amounts of the "free" and associated hydroperoxide anions, whereas the changes at higher NaOH concentrations are likely to also involve the effects of strong dehydration on the energies of ground and excited states of one or both absorbing species. For the lower range of NaOH concentration, the association constant of the hydroperoxide anion with the Na^+ cation and the electronic spectrum of the ($Na^+HO_2^-$) ion pair could be directly determined from the BIMSA fitting.

Acknowledgment. Financial support from Industrial Materials for the Future (IMF) Program of the Office of Industrial Technologies of DOE is gratefully acknowledged. The authors also thank Amanda Casteel for the peroxide determination in some NaOH samples.

References and Notes

(1) Otsuka, K.; Yamanaka, I. *Electrochim. Acta* **1990**, 35, 319.

(2) Yamanaka, I.; Hashimoto, T.; Otsuka, K. *Chem. Lett.* **2002**, 852.

(3) Lewdorowicz, W.; Tokarz, W.; Piela, P.; Czerwinski, A. *Przem. Chem.* **2005**, *84*, 858.

(4) Liu, W.; Zuckerbrod, D. *J. Electrochem. Soc.* **2005**, *152*, A1165 and references therein.

(5) Moorhouse, J., Ed. *Modern Chlor-Alkali Technology*; Blackwell Science: London, 2001.

(6) Lipp, L.; Gottesfeld, S.; Chlistunoff, J. *J. Appl. Electrochem.* **2005**, *35*, 1015.

(7) Muhammad, S. S.; Rao, T. N. *J. Chem. Soc.* **1957**, 1077.

(8) (a) Blum, L.; Bernard, O. *J. Stat. Phys.* **1995**, *79*, 569. (b) Bernard, O.; Blum, L. *J. Chem. Phys.* **1996**, *104*, 4746.

(9) (a) Percus, J. K.; Yevick, G. *Phys. Rev.* **1964**, *136*, 290. (b) Lebowitz, J. L.; Percus, J. K. *Phys. Rev.* **1966**, *144*, 251. (c) Waisman, E.; Lebowitz, J. L. *J. Chem. Phys.* **1970**, *52*, 4307.

(10) (a) Blum, L. *Mol. Phys.* **1975**, *30*, 1529. (b) Blum, L.; Høye, J. S. *J. Phys. Chem.* **1977**, *81*, 1311.

(11) (a) Wertheim, M. S. *J. Chem. Phys.* **1986**, *85*, 2929. (b) Wertheim, M. S. *J. Chem. Phys.* **1987**, *87*, 7323. (c) Wertheim, M. S. *J. Chem. Phys.* **1988**, *88*, 1214. (d) Wertheim, M. S. *J. Stat. Phys.* **1984**, *35*, 19. (e) Wertheim, M. S. *J. Stat. Phys.* **1986**, *42*, 459.

(12) (a) Simonin, J. P.; Bernard, O.; Blum, L. *J. Phys. Chem. B* **1998**, *102*, 4411. (b) Simonin, J. P.; Bernard, O.; Blum, L. *J. Phys. Chem. B* **1999**, *103*, 699.

(13) Vilariño, T.; Bernard, O.; Simonin, J. P. *J. Phys. Chem. B* **2004**, *108*, 5763.

(14) Bouby, M.; Billard, I.; Duplâtre, G.; Simonin, J. P.; Bernard, O.; Brunette, J. P.; Goetz-Grandmont, G. *Phys. Chem. Chem. Phys.* **1999**, *1*, 3765.

(15) Schumb, W. C.; Satterfield, C. N.; Wentworth, R. L. *Hydrogen Peroxide*; Reinhold Publishing Corporation: New York, 1955; p 566.

(16) Aziz, F.; Mirza, G. A. *Talanta* **1964**, *11*, 889.

(17) Mackerell, A. D., Jr. *J. Comput. Chem.* **2004**, *25*, 1584.

(18) Levine, I. N. *Quantum Chemistry*; Prentice Hall: Upper Saddle River, NJ, 2000.

(19) Simonin, J. P.; Blum, L.; Turq, P. *J. Phys. Chem.* **1996**, *100*, 7704.

(20) Blandamer, M. J.; Fox, M. F. *Chem. Rev.* **1970**, *70*, 59.

(21) Evans, M. G.; Uri, N. *Trans. Faraday Soc.* **1949**, *45*, 224.

(22) Chen, C.-P.; Tilak, B. V. *J. Appl. Electrochem.* **1996**, *26*, 235.

(23) Treinin, A.; Yacoobi, M. *J. Phys. Chem.* **1964**, *68*, 2487.

(24) Buser, W.; Hänisch, H. *Helv. Chim. Acta.* **1952**, *35*, 2547.

(25) Carrell Morris, J. *J. Phys. Chem.* **1966**, *70*, 3798.

(26) Nakagawara, S.; Goto, T.; Nara, M.; Ozawa, Y.; Hotta, K.; Arata, Y. *Anal. Sci.* **1998**, *14*, 691.

(27) Friedman, H. L. *J. Chem. Phys.* **1953**, *21*, 318.

(28) Emmenegger, F.; Gordon, G. *Inorg. Chem.* **1967**, *6*, 633.

(29) Sassella, A.; Borghesi, A.; Spearman, P.; Tavazzi, S. *Eur. Phys. J. B* **2002**, *28*, 385.

(30) Griffiths, T. R.; Wijayanayake, R. W. *Chem. Phys. Lett.* **1980**, *72*, 301.

(31) Sawyer, D. T. *J. Phys. Chem.* **1989**, *93*, 7977.

(32) Loeff, I.; Treinin, A.; Linschitz, H. *J. Phys. Chem.* **1992**, *96*, 5264 and references therein.

(33) Stein, G.; Treinin, A. *Trans. Faraday Soc.* **1959**, *55*, 1086.

(34) Jortner, J.; Raz, B.; Stein, G. *J. Chem. Phys.* **1961**, *34*, 1455.

(35) Treinin, A.; Wilf, J. *J. Phys. Chem.* **1970**, *74*, 4131.

(36) Ramond, T. M.; Blanksby, S. J.; Kato, S.; Bierbaum, V. M.; Davico, G. E.; Schwartz, R. L.; Lineberger, W. C.; Ellison, G. B. *J. Phys. Chem. A* **2002**, *106*, 9641.

(37) Castet, S.; Dandurand, J.-L.; Schott, J.; Gout, R. *Geochim. Cosmochim. Acta* **1993**, *57*, 4869.

(38) Fournier, O.; Oelkers, E. H.; Gout, R.; Pokrovski, G. *Chem. Geol.* **1998**, *151*, 69.

(39) *Handbook of Chemistry and Physics*, 84th Edition; CRC Press, LLC: Boca Raton, FL, 2004; pp 6-154−6-155.

(40) Highly concentrated NaOH solutions containing large quantities of peroxide produced a yellowish solid upon evaporation under ambient conditions at Los Alamos elevation (∼2100 m). The origin of the coloration has not been determined.

(41) Grehl, M.; Fröhlich, R.; Thiele, S. *Acta. Crystallogr., Sect. C* **1995**, *51*, 1038.

(42) Krom, J. A.; Petty, J. T.; Streitwieser, A. *J. Am. Chem. Soc.* **1993**, *115*, 8024.

(43) Balej, J. *Int. J. Hydrogen Energy* **1984**, *10*, 233.